DISSERTATION

NUMERICAL SIMULATIONS OF $Cu(In,Ga)Se_2$ SOLAR CELLS

Submitted by

Markus Gloeckler

Department of Physics

In partial fulfillment of the requirements

For the Degree of Doctor of Philosophy

Colorado State University

Fort Collins, CO

Summer 2005

Contents

List of Figures

List of Tables

Symbols

A	diode quality factor	
ΔE_C	conduction-band offset	[eV]
ΔE_V	valence-band offset	[eV]
ΔE_{Ba}	band-gap increase toward the back	[eV]
ΔE_{Fr}	band-gap increase toward the front	[eV]
$\mathcal{E}$	electric field	[V/cm]
ϵ	electric permittivity; ϵ/ϵ_0 = dielectric constant	[F/m]
E_C	conduction-band minimum	[eV]
E_{fn}	electron quasi-Fermi level	[eV]
E_{fp}	hole quasi-Fermi level	[eV]
E_V	valence-band maximum	[eV]
FF	fill factor	[%]
Φ	photon flux density	[#/cm^{2}s]
ϕ_{gb}	electrostatic grain-boundary potential	[eV]
η	solar-cell efficiency under one-sun illumination	[%]
J_0	diode saturation current density	[mA/cm^2]
J_{sc}	short-circuit current density	[mA/cm^2]
μ_e, μ_h	electron and hole mobility	[cm^2/Vs]
n	free electron density	[cm^{-3}]
N_A	bulk absorber doping	[cm^{-3}]
N_{gb}	density of grain-boundary states	[cm^{-2}]
p	free hole density	[cm^{-3}]
q	elementary charge	[C]
R_{bulk}	bulk recombination rate	[cm^{-3}s^{-1}]
R_F	front reflection	[%]
R_{gb}	GB recombination rate	[cm^{-2}s^{-1}]
S_{gb}	GB recombination velocity	[cm/s]
τ_e, τ_h	electron and hole lifetime	[s]
V_{oc}	open-circuit voltage	[V]
W_{gb}	distance between two columnar GBs = "grain size"	[cm]
W_{SCR}	width of the space-charge region	[cm]
W_{QNR}	width of the quasi-neutral region	[cm]

Abbreviations

AM1.5	standard terrestrial solar spectrum 'Air Mass 1.5'
CBO	conduction-band offset
CE	collection efficiency
CGS	$CuGaSe_2$
CIGS	$Cu(In,Ga)Se_2$
CIS	$CuInSe_2$
GB	grain boundary
J-V	current-density vs. voltage [curve]
one-sun	used as a synonym for AM1.5 illumination
PV	photovoltaic
PX	poly-crystalline
QE	quantum efficiency
QNR	quasi-neutral region
SCR	space-charge region
SEM	scanning electron microscopy
SRH	Shockley-Read-Hall (recombination)

Chapter 1

Motivation

From the dictionary [1]:

solar cell:	*a photovoltaic cell that converts sunlight directly into electricity.*
thin film:	*a film of material only a few microns thick, deposited on a substrate, as in the technology for making integrated circuits.*

Why bother?

Only after having worked on thin-film solar cells for some time and after I had exposure to the thin-film photovoltaic (PV) community and also to the political aspects that come with it, did I ask this question myself. Before that time, solar cells were simply inherently "cool", as they are obviously something "very green", produce a high form of energy out of nowhere, and with virtually no effort. Now there are a few inaccuracy in this early perception that need to be addressed: First off, energy is not produced by solar cells, but, of course, merely converted. On the other hand, conversion off something that is naturally lost, i.e., sunlight hitting the earth, appears very much as a net gain (or "production"). Further and more important questions are: (1) Is PV really "green" and is it "green enough" that we need to care about it? (2) Can PV really make an impact? (3) And an impact on what and if so, is it for economic, ecological, or political reasons?

Photovoltaics today

The PV industry has grown into a multi-billion dollar business and production of PV modules (= "large area conglomerate of solar cells") exceeds hundreds of MWs, surpassed the 1 GW for the first time in 2004 and is expected to reach 3 GW by 2010 [2]. The market has been growing at double digit rates over recent years (20–40% annually) [2, 3] and prices, usually referred to in dollars per peak Watt ($/Wp), are continuously falling, roughly with a "learning curve" of 80% (i.e., Ref. [4]), Figure 1.1. A further increase of cumulative production by a factor of 100 will lead to a cost equality with fossil fuels. This can expected to occur in roughly 15 years, if the technology is able to follow the 80% learning curve. Unfortunately, learning curves tend to experience a "change in slope" once a technology is sufficiently matured and prices stabilize, similarly as it was seen for gas or wind turbines in the early 1960 and 1990, respectively [4]. Photovoltaic crystalline silicon technology is likely to hit this lower price limit significantly earlier due to expensive processing and materials involved, which makes thin-film solar cells the more promising candidate for huge-scale production.
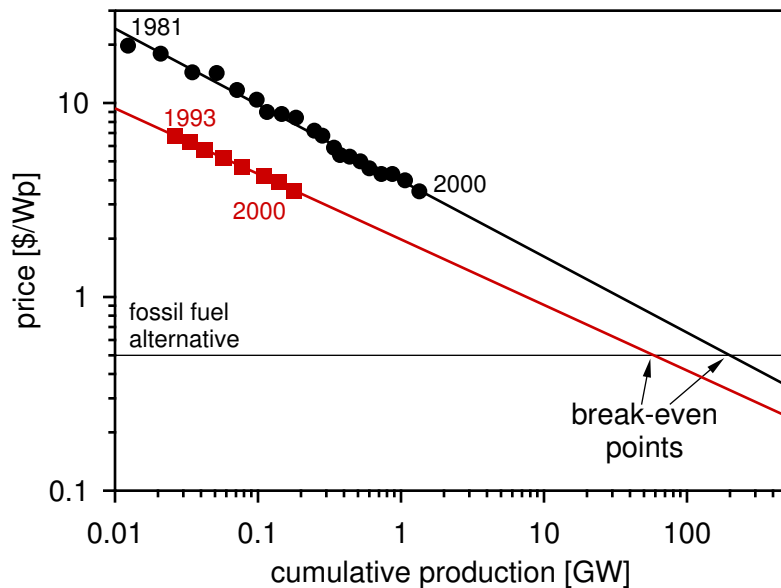
Figure 1.1: Learning curve of photovoltaics. Thin-films have a significant cost advantage as the learning curves starts from a lower base. Compared to Si technology, thin-films achieve similar total costs at substantially lower production volumes. [Data assembled by Jun Pan, Colorado State University].

Todays economic success of PV is important as it fosters future developments, but crucially depends on political incentives such as "feed-in tariffs", as they have been established in several European countries (i.e., Ref. [5]), installation subsidies, or high electricity costs in general. *Thin-film* solar cells have currently less than 10% market share in PV module shipments, which is dominated by crystalline Si technology. The overall electricity production from solar installations is still entirely negligible in comparison to the world energy demand. However, taking the incentives as granted or under consideration of the high electricity costs in parts of the world, i.e., Japan, photovoltaic energy is a highly competitive and lucrative market today. This caused a total depletion of the solar module market and great rush toward increasing the production capacity in 2004.

Coming back to the "green aspect" of photovoltaic energy conversion. PV is an inherently clean form of energy once it is installed in the field. Solar cells convert the incident solar radiation directly into electricity, requires no fuel, and produces no exhausts or other bi-products. However, in order to be a sustainable clean form of energy, one also needs to consider what is necessary to produce a solar panel. Other frequent objections to solar power are that they require huge land areas and we probably will not have enough rare materials to produce substantial amounts of solar cells anyway.

The question of sustainability requires that solar modules "generate" substantially more energy during their estimated 30 year lifespan compared to what was necessary in the manufacturing process of the solar panel in the first place. For current Si technologies this "pay back" time is estimated roughly at 3–4 years, for thin-films 3 years or less, both numbers include the total system cost [6]. These numbers are anticipated to further decrease to as low as 2 years for Si and 1 year or less for thin-films. Silicon and most other materials are readily available for any amount of solar panel production one could foresee, some materials, such as Indium in $Cu(In,Ga)Se_2$ solar cells could become a bottleneck, if the production would eventually reach TW levels [7]. The land area necessary to produce solar power is in general grossly overestimated. Roughly 0.25 TW of electricity could be generated by building integrated PV, i.e., on roofs (Fig. 1.2), and 1.7% of the US land area would generate as much as 3.3 TW, which is approximately the *total* energy consumption in the US in 2000. This land area is similar to what is used for interstate highways, which proofs

Figure 1.2: Building integrated PV installation on a farm house in the author's home town. This installation After the passing of the Renewable Energy Law in Germany, many private investors use this opportunity to invest in solar energy with practically guaranteed return and profits on investments.

that if the necessity is established, a project of this size can be accomplished.

To summarize the current situation, the solar-cell market is a highly lucrative at the moment due to guaranteed feed-in tariffs and high electricity prices in parts of the world. The learning curves predict further substantial price reductions as the market grows at rates of 20–40%. Other than economic consideration, there are no constrains in sight that will limit the success of solar energy. State-of-the-art thin-film solar cells have been recently reviewed [8, 9].

Photovoltaics 2050

With our ever increasing industrialization and growth in world population, we, as in "humanity" or at least "those that we live on earth", may face major challenges in the future energy demand. Only the tip of the iceberg will be presented here and for in depth discussion the reader is referred to recent publications of the National Renewable Energy Laboratory [10] and the World Energy Assessment [11] and discussion by Hoffert et al. [12] and Lewis [13]. By 2050, the average power demand is expected to increase, mostly due to the increase in world population, from 13 TW (2000) to roughly 30 TW. Our current energy mix is heavily focused on fossil fuels and there is no end in sight, since reserves for fossil fuels,

particularly coal, are sufficient to meet this future demand.

The driving factor for renewable energies will become the increased level of greenhouse gas emissions, particularly CO_2 that accumulates in our atmosphere. The atmospheric CO_2 concentration has raised from roughly 280 parts per million (ppm) to 360 ppm [11] since the late 19th century. Increases to 450–550 ppm are predicted to cause major climatic changes. At the current rate of fossil fuel consumption and assuming the increased global energy demand will be faced with fossil fuels as well, the CO_2 concentration is predicted to raise as high as 750 ppm by 2050, tripling the pre-industrial concentration [13]. In this scenario, the planet earth could very quickly become a less habitable place to live, the world population would decline and, of course, might alleviate some of the energy demand problem.

The alternative to the "business as usual" approach, requires that we reduce the CO_2 emission over the next few decades and that we are ready to supply a good portion of the energy demand (10–30 TW) by 2050 using renewable, emission-free energy sources. Lewis [13] reviews possible candidates for clean energy production, including nuclear fission, hydropower, biomass, wind, geothermal, and solar energy and finds that solar power is the only source that has the potential to face this demand. While, hydro, biomass, geothermal, and wind power can sustain fractions of this demand, for practical purposes the maximum power supplied by these techniques will be limited. Nuclear fission, has the potential to supply CO_2-free power, but it would require to built one nuclear 1 GW reactor every other day to meet the 10 TW demand in 2050, and even if this could be accomplished, we might run out of uranium on a rather short time scale. Solar energy is incident on earth at a rate of $\sim 10^5$ TW and offers great potential to meet this increased demand in CO_2-free energy. The high costs associated with PV, however, requires that political driving forces are establish to enable the necessary growth of the technology. The realization of this global goal will require a concerted effort throughout the world and across borders.

The question at hand is not whether humanity should or will use solar power, but rather what alternatives are available to face our energy future. Solar power offers a great clean opportunity at hand and unless others become available, it might be the only one that can prevent climatic catastrophes that we will face before the end of this century.

Chapter 2

Background

Important principles and properties of semiconductors and solar cells are briefly reviewed as far as these are helpful for the understanding of this work. This includes a brief description of state-of-the-art Cu(In,Ga)Se$_2$ (CIGS) solar cells. Although this work is focused on numerical simulations of solar cells, it is essential to review basic measurement principles as well, because it is exactly the results of these measurements that are calculated in numerical simulations. The discussion is limited to current density vs. voltage (J-V) and quantum efficiency (QE) measurements.

2.1 Solar cell basics

2.1.1 Important semiconductor concepts

Semiconductors are a family of solids in which there exists a moderate gap (up to a few electron volts) in the distribution of allowed energy states and at T = 0 K this gap separates one entirely filled band (valence band) from one that is entirely empty (conduction band). For T > 0 K, a finite number of electronic states are occupied in the conduction band ("free electrons") and a finite number of states are unoccupied in the valence-band ("free holes"). These free electrons and holes can gain kinetic energy since a quasi-continuum of higher (electrons) or lower (holes) states are available to them and, therefore, they are able to respond to electric fields and concentration gradients and allow for macroscopic current flow.

The equilibrium concentration of electron and holes can be affected by external dopants, but also by defect levels (additional states within the band gap) that are intrinsic to the materials. The occupation of the conduction and valence band is governed by Fermi-Dirac statistics,

$$F(E) = \frac{1}{1 + exp\left(\frac{E - E_f}{kT}\right)} \tag{2.1}$$

where k is the Boltzmann's constant and T the absolute temperature. Equation 2.1 describes the probability to find electrons in the conduction band and, similarly, 1-$F(E)$ describes the probability for holes in the valence band. If the Fermi-level E_f is not very close to either band edge, $E_C - E_f \gg kT$ and $E_f - E_V \gg kT$, $F(E)$ can for many practical purposes be replaced by Boltzmann factors such as

$$exp\left(-\frac{E - E_f}{kT}\right) \quad \text{and} \quad exp\left(-\frac{E_f - E}{kT}\right) \tag{2.2}$$

for electrons in the conduction band and holes in the valence band, respectively.

Materials are classified as n and p-type semiconductors depending on majority of electron or hole carriers. The Fermi level in doped semiconductors can be calculated by the following relations:

$$n = N_C \cdot exp\left(-\frac{E_C - E_F}{kT}\right) \tag{2.3}$$

$$p = N_V \cdot exp\left(-\frac{E_F - E_V}{kT}\right) \tag{2.4}$$

where

$$N_C = 2\left(\frac{2\pi m_e^* kT}{h^2}\right)^{3/2} \quad \text{and} \quad N_V = 2\left(\frac{2\pi m_h^* kT}{h^2}\right)^{3/2} \tag{2.5}$$

are the effective density of states in the conduction and valence-band. All parameters in Eq. 2.5 have their usual meaning, m_e^* and m_h^* are the electron and hole effective masses. In equilibrium, the product of n and p is a constant and depends only upon the temperature, effective masses, and band gap of the semiconductor.

$$np = n_i^2 = N_C \cdot N_V \cdot exp\left(-E_g/kT\right) \tag{2.6}$$

Non-equilibrium

In non-equilibrium conditions, such as under illumination or under carrier injection due to externally applied electric bias, no uniform Fermi level exists. If the situation is in a steady-state condition, however, quasi-Fermi levels can be introduced, which are similarly useful in the analysis and interpretation of semiconductors. These quasi-Fermi levels are defined by:

$$n = N_C \cdot exp\left(-\frac{E_C - E_{fn}}{kT}\right) \tag{2.7}$$

$$p = N_V \cdot exp\left(-\frac{E_{fp} - E_V}{kT}\right). \tag{2.8}$$

Assuming that E_{fn} and E_{fp} are in equilibrium with the electrical contacts to n and p-type materials in a p-n junction diode, the splitting of the quasi-Fermi levels in the proximity of the SCR equals the applied voltage V and it follows that the np product is voltage dependent:

$$np = n_i^2 \cdot exp\left(qV/kT\right) \tag{2.9}$$

Numerical solution to the p-n junction problem, including generation, recombination, and transport, is discussed in Sect. 3.1. Further information on the properties of semiconductors can be found in many semiconductor [14] or solar-cell text books [15, 16, 17].

2.1.2 Homo-junctions

Intimate contact between n and p-type semiconductors allows for exchange of electrons and holes until an equilibrium situation is achieved. Electrons diffuse into the p-type material, leaving behind ionized shallow donor levels, and holes diffuse into the n-type material, leaving behind ionized shallow acceptor levels. Adjacent to the p-n interface, both semiconductor deplete of free carriers and a space-charge region (SCR) is established. This is shown in Fig. 2.1(a) for a p-n homo-junction assuming a n and p doping of 10^{16} cm^{-3}. The diffusion process stops once the drift current established by the electric field, Fig. 2.1(b), exactly cancels the diffusion current and a flat Fermi level is established throughout the device. It is conventional to draw the conduction and valence-band edges in terms of the
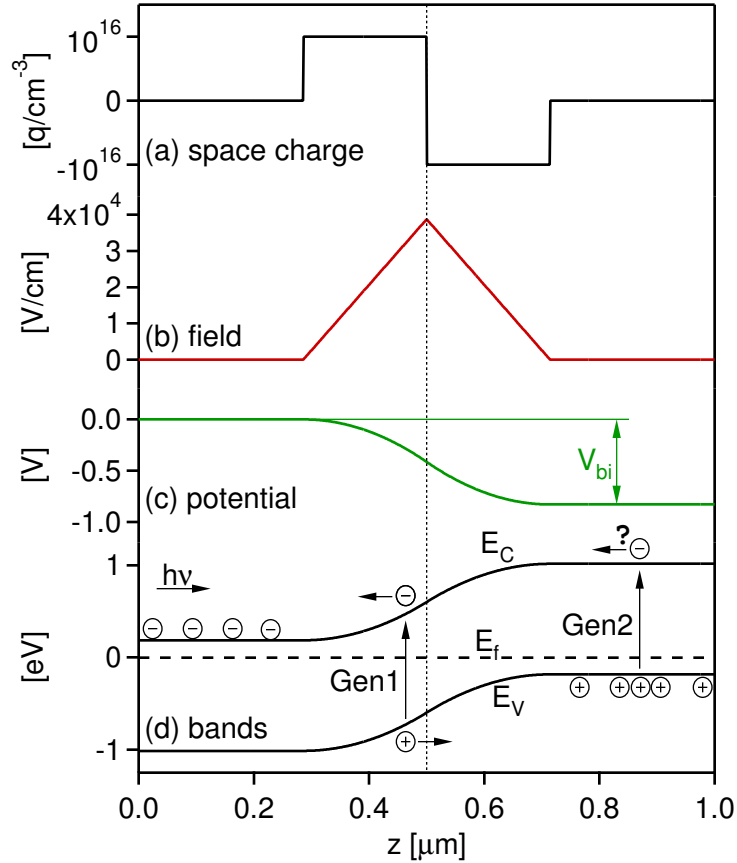
Figure 2.1: Formation of a *p-n* junction in the Schottky approximation. (a) space-charge distribution due to fixed ionized dopants; (b) electric field obtained by integration of the Poisson equation; (c) another integration step results in the electrostatic potential. The built-in potential V_{bi} describes the potential difference between the n and p side of the junction in equilibrium. Collection of photo-carriers requires that the applied voltage $V < V_{bi}$ and, therefore, V_{bi} is an upper limit to the open-circuit voltage of a solar cell (Sect. 2.2.1); (d) conduction-band minimum E_C, valence-band maximum E_V, and the Fermi level in equilibrium. Schematically the generation of an electron hole pair within (Gen1) and outside (Gen2) the space-charge region is shown.

electron energy and, hence, the electrostatic potential $\phi = -E_C +$ (constant) (Fig. 2.1[c] and [d]).

Figure 2.1(d) further illustrates the principle of a *p-n* junction solar cell. Incident light (from the left) generates additional electron-hole pairs in the solar cell. If the generation occurs within the SCR, both carriers are readily swept out by the electric field (process "Gen1" in Fig. 2.1[d]). The hole quickly reaches the *p*-type region and the electron the *n*-type region; once both carriers are majority carriers, they can then safely transverse through the quasi-neutral region (QNR) and be eventually collected at external electrical contacts.

In case of generation outside of the SCR, either in the n or p-type bulk material (illustrated in "Gen2" in Fig. 2.1[d]), one of the two generated carriers is a minority carrier (electron in Fig. 2.1[d]) and has to transverse to the SCR before it recombines; the likelihood of this diffusion transport to succeed depends on quality of the material and is often expressed in terms of a carrier lifetime τ or a diffusion length L.

2.1.3 Hetero-junctions

The situation of a p-n homo-junction solar cell depicted in Fig. 2.1(d) is far from ideal, because the generation of light reduces exponentially with the penetration depth (Sect. 3.1.3) and, therefore, assuming the light would be incident from the n-type side of the solar cell, most of the generation would occur in the n-type QNR region and not within the SCR where good collection would be ensured.

There are two effective approaches to improve upon this situation: (1) thinning of the n-type material and this approach is taken, i.e., in Si based solar cells, or (2) using a n-type material with an enlarged band-gap energy. The latter would shift the generation profile directly into the junction, since the large E_g will prevent absorption in the n-type layer, and form a very efficient solar cell. This is the concept of a hetero-junction solar cells such as ZnO/CdS/CIGS, which will be discussed in this work. The n-type layers are often referred to as "window" layers, due to their intended photon transparency.

The band diagram for a ZnO/CdS/Cu(In,Ga)Se$_2$ solar cell is shown in Fig. 2.2. Photons of energy >3.3 eV will pass through the ZnO window layer, some photons of energy 2.4 eV < E_{ph} < 3.3 eV are absorbed in the CdS buffer layers, which was introduced into these devices for technological reasons, but most will reach the CIGS layer and be strongly absorbed in the SCR. CIGS as well as CdTe are direct semiconductor with very strong absorption, such that the absorption length is very short, $\alpha^{-1} \ll 1$ μm. The detrimental CdS absorption is minimized by thinning this layer or alloying it with other elements which increases its band-gap energy [18].

Several important aspects of this band diagram will be discussed in Chapter 4.
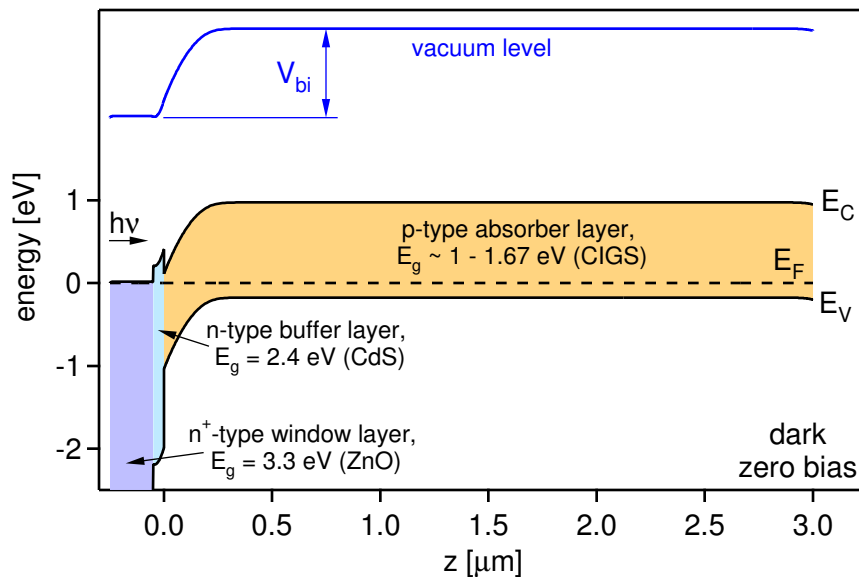
Figure 2.2: Conduction and valence band for a hetero-junction solar cell; the case of ZnO/CdS/CIGS.

2.1.4 Thin-film solar cells

Sunlight is incident on earth (at sea level) with a power density of $\sim$1000 W/m^2 and, hence, to run a standard 100 W light bulb by solar power, an area of roughly 1 m^2 is required (even more if the light bulb should run 24h or adverse weather is considered). For significant energy production, large-area solar-cell installations are necessary. In comparison to wafer based Si technology, thin-film solar cells can be cheaply deposited on large areas of (soda-lime) glass [19], stainless steel [20], or even on polyimide substrates, which would make these solar cells a true lightweight [21, 22]. An additional problem with traditional Si solar cells is that the required energy "pay back" time is on the scale of 2-3 years and, therefore, 10% of the lifetime of a Si solar panel is lost; thin-film solar cells are far less demanding and have the potential to achieve pay-back times of one year [6]. Lastly, in part a combination of the last two arguments, but also of many other contributing factors, thin-film solar cells have the potential to be significantly cheaper in large scale production. Recent studies have shown that the application of *todays technologies* in a "super-large scale" manufacturing of thin-film solar cells would lead to solar electricity prices that are competitive with conventional energy sources [23].

11

Typical Cu(In,Ga)Se$_2$ solar cells

Despite their polycrystalline nature, thin-film solar cells based on the chalcopyrite compounds of Cu(In,Ga)Se$_2$ (CIGS) achieve surprisingly high conversion efficiencies approaching 20% [24, 25, 26]. Besides the presence of grain boundaries (GBs), CIGS thin-films capable of achieving high efficiency substantially differ from single-crystals, particularly elemental semiconductors, in that they are always non-stoichiometric (Cu-poor) [25, 27], often non-uniform in the Ga/(Ga+In) composition throughout the film-thickness [25], can form defect complexes that are benign to device performance [28], and in most cases require the presence of sodium during growth or sodium introduced by post-deposition treatments [29].
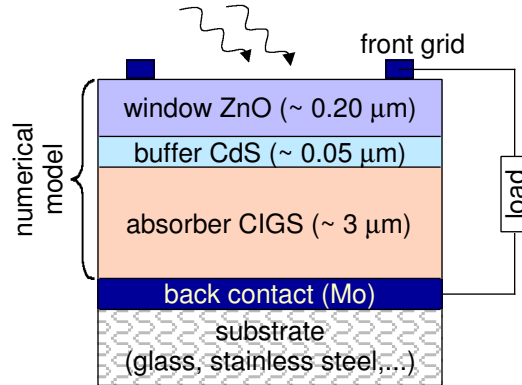
Figure 2.3: Schematic of a grid/ZnO/CdS/CIGS/Mo/glass solar cell. Only the semiconductor layers are reproduced in numerical models. The metallic contacts at the top and bottom are defined by their work function and surface recombination velocity. An external load is connected between negative (grid) and positive (Mo) electrode.

A typical device structure [19, 27] is shown in Fig. 2.3. CIGS solar cells are almost exclusively designed in a substrate configuration starting from soda-lime glass, stainless steel, or polyimide material. The back contact is typically sputtered Mo and forms a non-blocking contact with CIGS. In contrast, for example, in CdTe solar cells, the back contact forms Schottky barriers and represents a major hindrance in the commercialization due to stability issues [30].

The CIGS absorber material with typical thicknesses of 2–3 μm is deposited by a great variety of processes that can be roughly categorized [19, 27] into vacuum co-evaporation and two-step selenization processes. Co-evaporation deposits all elements simultaneously

on a heated substrate. Intentionally or un-intentionally, gradients in the composition can be created and it is investigated in Sect. 4.1 whether such gradients can be beneficial to device performance. Selenization processes deposit all metals onto a film and react them in Se atmosphere to form the intended compound. The patented "three- stage" processes, which makes the best CIGS solar cells to date [24], combines these two approaches by using vacuum deposition methods, but at the same time separating the metal deposition and selenization into two process steps by the variation of the elemental fluxes [25].

ZnO window and CdS buffer layers are deposited on top of the CIGS absorber by RF-sputtering and chemical bath deposition, respectively. A buffer layer, although not necessary from the basic consideration of a hetero-junction solar cell, has proven beneficial to device performance. ZnO layers are often realized in a bi-layer configuration of intrinsic and Al-doped material. A review of buffer and window layers and evaluation of possible alternatives was recently conducted by Pudov [31]. The effect of the band-alignment at the CdS/CIGS interface, is discussed in Sect. 4.2.

Figure 2.4: SEM image of a CIGS solar cell at 20000x magnification. In high quality material, grains extend throughout the film thickness. Image courtesy of K. Ramanathan, NREL.

A cross-sectional scanning electron microscopy (SEM) image of a ZnO/CdS/CIGS solar cell is shown in Fig. 2.4. This image was taken on a sample made at the National Renewable

Energy Laboratory that achieved 19.3% conversion efficiency [26]. From bottom to top: soda-lime glass, a double layer of Mo, roughly 2 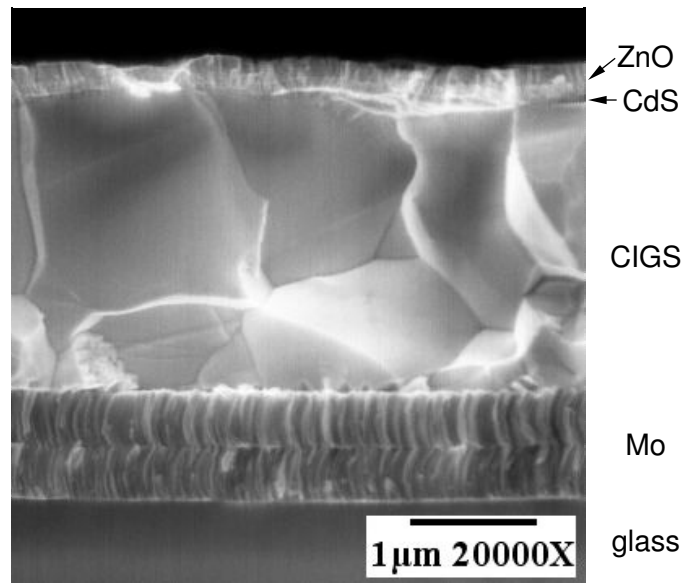μm of CIGS, 50 nm CdS (hardly visible in Fig. 2.4), and a double layer of intrinsic and doped ZnO. Noticeably, the grain widths are comparable to the film thickness, leading to a columnar film structure. In the top part of the CIGS layer, where the electronic junction is located, the material appears relatively immaculate and and free of macroscopic defects, particularly grain boundaries. At the beginning of the growth, at the Mo/CIGS interface, some additional GBs develop during crystallization. The effects of such horizontal and columnar grain boundaries on device performance are investigated using two-dimensional models in Chapter 5.

Broad reviews of the state-of-the-art thin-film solar cells was given in recent special edition of *Progress in Photovoltaic* [32, 33], several articles in the *Photon* magazine [8, 9], and in earlier work [27]. Several chapters in Ref. [17] are devoted to the discussion of a-Si, CdTe, and CIGS thin-film solar cells.

2.2 Electrical characterization methods

In the wide range of characterization methods available for thin-film solar cells, few are as misleading and yet as telling, as the measurement of current-density vs. voltage curves (J-V). Although it is of utmost importance as it determines the efficiency at which the solar cell converts the sun's power into electricity, the J-V curve itself could hardly tell less about the actual device or materials present in the device. One extension of a regular J-V measurement is the measurement of the wavelength-dependent current response, typically performed at zero bias. This is referred to as the "quantum efficiency" (QE) as it, after proper normalization, represents what fraction of photons of wavelength λ are efficiently converted into electron-hole pairs and collected. QE measurements under light or voltage bias, can be misleading and careful analysis is necessary [34, 35].

Numerical simulations of solar cells have the advantage that all device and material parameters are well controlled as they are input parameters of the model and, therefore, evaluation of trends and quantified changes in J-V or QE measurements are possible. Although, some tools also allow the simulation of capacitance related techniques [36, 37] this

is not addressed here and, therefore, also not discussed in the introduction.

2.2.1 Current density vs. voltage

The standard current-density vs. voltage measurement, often abbreviated as "current-voltage" or J-V, is performed at room temperature and under a standardized "one-sun" illumination [38]. Experimentally, it is necessary to cool the solar cell during illumination, as otherwise the intense illumination leads to an increase in the cell's temperature. For details of the set-up used in the Photovoltaic laboratory at Colorado State University see Refs. [39] and [31]. In short, the solar cell is subject to a calibrated light source, two contacts are used to apply a voltage bias, and two additional contacts are used to determine the resulting cell current.

An example of a J-V curve is shown in Fig. 2.5(a) and from such a curve, the basic performance parameters can be extracted as listed in Table 2.1. Assuming that the curve

Table 2.1: Basic J-V performance parameters. For ideal solar cells, which can be described by an exponential diode equation, these parameters are redundant, such that three of these are sufficient to specify performance.

Parameter	Symbol	Unit	Determined by
open-circuit voltage	V_{oc}	V	$J = 0$
short-circuit current density	J_{sc}	mA/cm^2	$V = 0$
max. power voltage	V_{max}	V	V at $(JV)_{max}$
max. power current	J_{max}	mA/cm^2	J at $(JV)_{max}$
fill factor	FF	%	$(V_{max}J_{max})/(V_{oc}J_{sc})$
efficiency	η	%	$(JV)_{max}/P_{incident}$

follows an exponential behavior, there is redundancy in these parameters and only three (i.e., V_{oc}, J_{sc}, η) are necessary to specify them all.

Ideally, a J-V curve resembles an ideal diode curve shifted by the light current $J_L \simeq J_{sc}$:

$$J(V) = J_0 \left[exp\left(\frac{qV}{kT}\right) - 1 \right] - J_L. \tag{2.10}$$

However, application of this equation to thin-film solar cells requires that parasitic losses
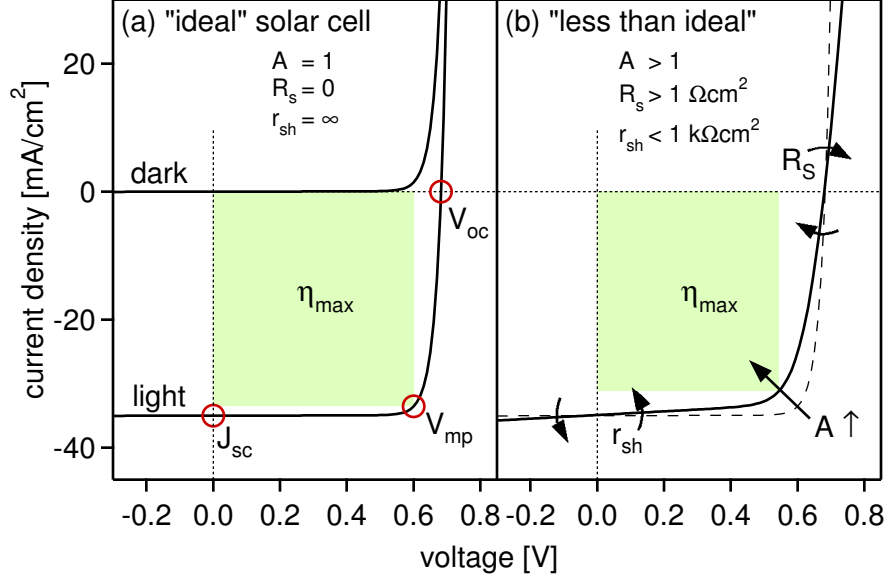
Figure 2.5: (a) jv curve for an ideal solar cells; standard J-V parameters that describe performance of a solar cells. (b) Non-ideal behavior includes parasitic resistances and a diode quality factor greater unity.

are included [40]:

$$J(V) = J_0 \left[exp\left(\frac{q(V - R_S J)}{AkT} \right) - 1 \right] + \frac{V - R_S J}{r_{sh}} - J_L. \tag{2.11}$$

Series resistance R_S, shunt-resistance r_{sh}, and diode quality factor A describe these non-idealities. The effect of each of these parameters on the J-V curve is shown in Fig. 2.5(b). In record efficiency cells [24], R_S and r_{sh} effects are negligible, and the best diode quality factors achieved are around 1.3. More typical values for these parameters are $R_S \sim 1$ Ωcm^2, $r_{sh} > 500$ Ωcm^2, and $A \sim 1.5$. The J-V curve analysis used in this work follows the procedure outlined by Hegedus and Shafarman [40], which includes the improved determination of the diode quality and series resistance suggested by Sites and Mauk [41]. The analysis process is illustrated in Fig. 2.6(a)-(d).

(a) Standard J-V curve results in V_{oc}, J_{sc}, FF, and η as given in Table 2.1.

(b) Plot of dJ/dV determines the shunt conductance, $G = 1/r_{sh}$, as shown in Fig.2.6(b).

(c) A plot of $dV/dJ = R + AkT/q(J + J_L)^{-1}$ versus $(J + J_{sc})^{-1}$ intercepts the y axis at
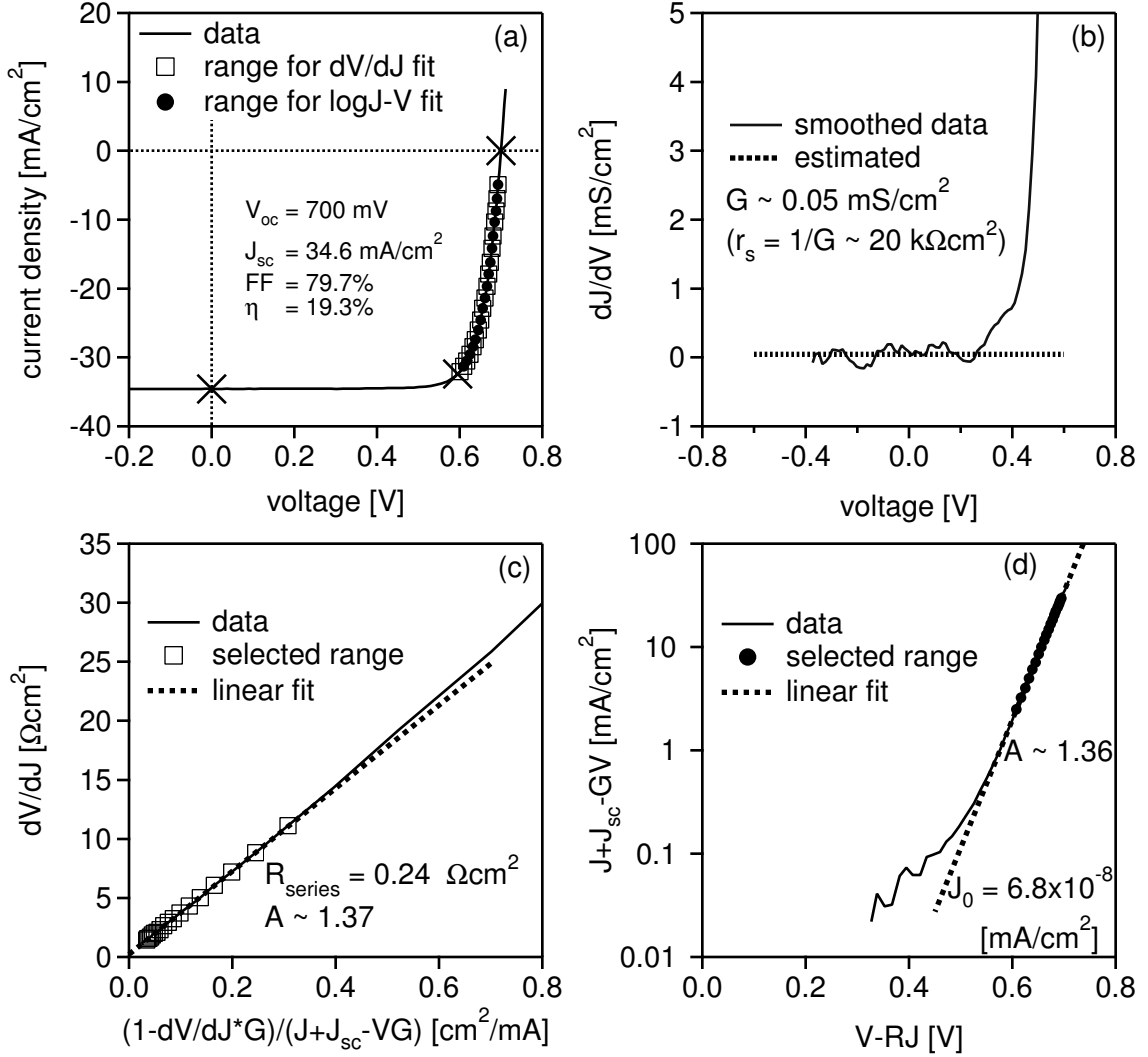
Figure 2.6: Four step analysis of *J-V* curves. The details of these four steps are given in the text. The curve shown is a 19.3% solar cell made at NREL [26], data courtesy of K. Ramanathan.

a value of R_S and the slope of the linear region allows to identify A.

(d) *J-V* plotted on a logarithmic scale, after correction for R_S and r_{sh}, allows to determine A by an alternative method. For well-behaved devices this A agrees well with the A found in step (c).

The results of the numerical simulations presented in Chapter 4 and 5 were subjected to this analysis procedure. A software application, named **Cur**rent-**V**oltage **A**nalysis (CurVA), was written that allows interactive analysis following the above outlined steps

with ease. A screen shot of this application is shown in Fig. 2.7. This program also re-placed a previous program used in the Photovoltaic laboratory at Colorado State University and is now in use by a number of other groups in the photovoltaic community working on CdTe, CIGS, or organic solar cells [24, 42].
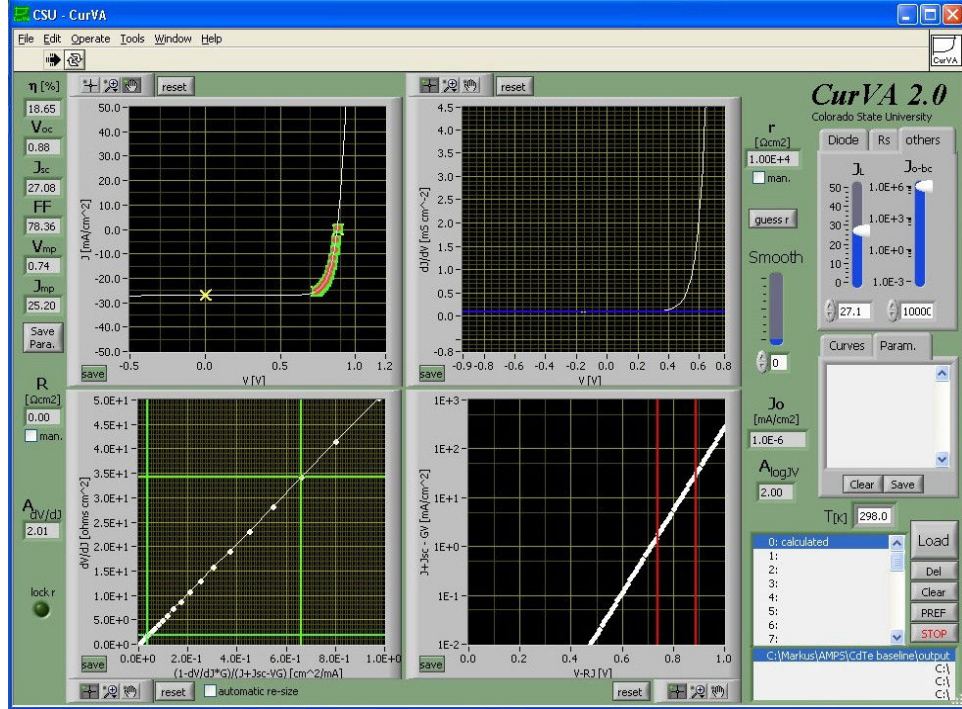
Figure 2.7: Four-step *J-V* analysis. The layout and implementation follows the discussion and figure in Ref. [40]. The analysis is performed in the four steps described above (from top left to bottom right). The evaluation ranges for the linear fits can be chosen by dragging of cursor lines in the displayed graphs, with immediate response. CurVA 2.0 includes import filters for seven different file formats and an automatic capturing of the analysis. As an additional feature, CurVA can calculate arbitrary *J-V* curves based on the paramters J_0, A, J_L, R_S, and r_{sh}.

2.2.2 Quantum efficiency

Measurement of the current response at zero volt and normalization of this current to the incoming photon flux, allows to calculate the quantum efficiency of a solar cell:

$$QE(\lambda) = \frac{\Delta J/q}{\Phi} = \frac{\#\text{collected electron-hole pairs}}{\#\text{incident photons}} \tag{2.12}$$

The optical excitation of flux density Φ is monochromatic and varies over the spectral range that is relevant to the solar cell application. Experimentally, the beam intensity varies as it scans through all wavelengths; in numerical simulations $\Phi = 10^{15}$ cm^{-2}s^{-1} is used which is a typical average number. More details on the experimental set-up is given elsewhere [31, 39].
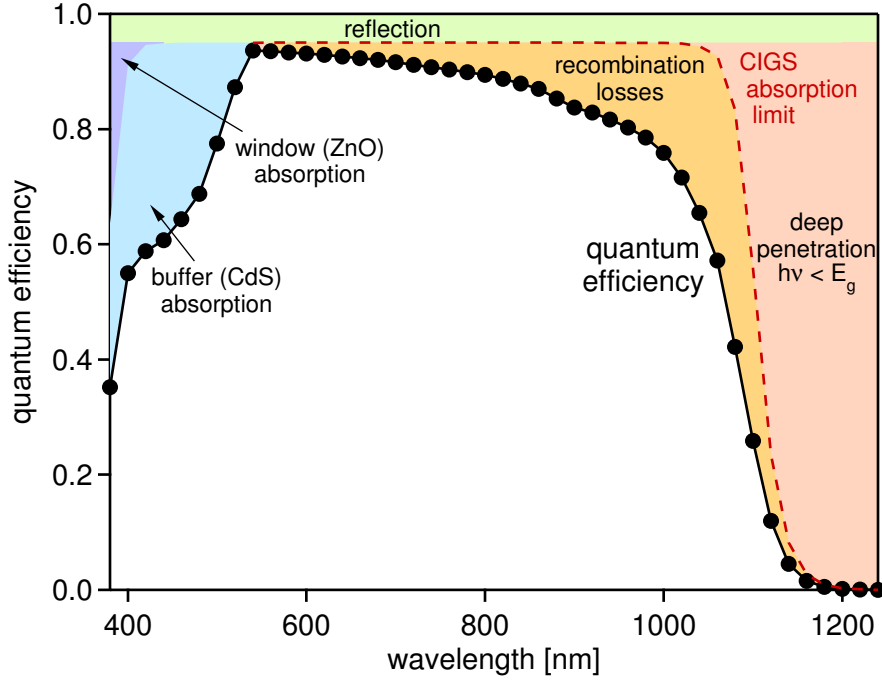
Figure 2.8: Example of a quantum-efficiency (QE) curve and involved loss mechanisms.

An example QE curve is shown in Fig. 2.8. This is the result of an numerical simulation, and, hence, a somewhat idealized case, but the differences to experimental QE curves will be addresses in the following:

- "Reflection" losses are introduced by partial coverage of the front surface by non-transparent contacts (i.e., metal contact fingers) or by reflection due to optical interference in the transparent conductive oxide layer. Experimentally, these losses are minimized by the application of anti-reflective coatings.

- "Window" absorption in the short-wavelength region is a negligible effect due to the high band-gap energy of this material. Free electron absorption in the ZnO layer can lower the quantum efficiency in the high wavelength region, but this effect is typically

small and neglected in the numerical simulations.

- "Buffer" absorption represents one of the major losses in current CIGS and CdTe thin-film solar cells. Thinning of the CdS or replacing it with a higher band-gap material are possible alternatives.

- "Recombination" losses are introduced by less-than-ideal collection efficiencies of photo-generated carriers. The longer the wavelength, the deeper the generation of carriers, and the higher the likelihood of recombination. This will be investigated in some detail in Sect. 5.3.4.

- "Deep penetration" of carriers. These losses are inherent to every semiconductor as light with photon energy of $h\nu < E_g$ is not absorbed.

The resulting QE curve in Fig. 2.8 is similar to QE curves observed in CIGS solar cells of good efficiency [40].

Bibliography

[1] *Random House Unabridged Dictionary, Copyright © 1997, by Random House, Inc., on Infoplease*, URL `www.infoplease.com`.

[2] Solarbuzz, *Marketbuzz 2005: Annual world solar photovoltaic (pv) market report*, URL `http://www.solarbuzz.com/Marketbuzz2005-intro.htm`.

[3] T. Surek, in *Proc. 3rd World Conf. Photovoltaic Energy Conversion* (2003), pp. 8PL–E3–01.

[4] M. A. Green, in *Proc. 3rd World Conf. Photovoltaic Energy Conversion* (2003), pp. OPL–02.

[5] Bundesministerium für Umwelt, Naturschutz und Reaktorsicherheit, *Gesetz zur Neuregelung des Rechts der Erneuerbaren Energien im Strombereich*, URL `http://www.bmu.de/erneuerbare/energien/doc/5982.php`.

[6] National Renewable Energy Laboratory, *What is the energy payback for PV?*, URL `http://www.nrel.gov/docs/fy04osti/35489.pdf`.

[7] N. R. E. Laboratory, *Will we have enough materials for energy-significant pvproduction?*, URL `http://www.nrel.gov/docs/fy04osti/35098.pdf`.

[8] K. Zweibel, H. Ullal, and B. von Roedern, *Finally: Thin-film PV!*, PHOTON International pp. 48–54 (October 2004).

[9] K. Zweibel, H. Ullal, and B. von Roedern, *Thin films in detail*, PHOTON International pp. 46–52 (November 2004).

[10] K. Zweibel, *Thin Film Solar Cells: Fabrication, Characterization and Applications* (John Wiley & Sons, 2005), chap. The terawatt challenge for thin-film PV, to be published.

[11] United Nations Development Programme, United Nations Department of Economic and Social Affairs, and World Energy Council, Tech. Rep. (2000), URL `http://www.undp.org/seed/eap/activities/wea/`.

[12] M. I. Hoffert, K. Caldeira, G. Benford, D. R. Criswell, C. Green, H. Herzog, A. K. Jain, H. S. Kheshgi, K. S. Lackner, J. S. Lewis, et al., Science **298**, 981 (2002).

[13] N. S. Lewis, *Global Energy Perspective*, URL `http://www.its.caltech.edu/~mmrc/nsl/energy.html`.

[14] S. M. Sze, *Physics of Semiconductor Devices* (John Wiley & Sons, 1981), 2nd ed.

[15] M. A. Green, *Solar Cells* (Prentice Hall, Englewood Cliff, NJ, 1982).

[16] A. L. Fahrenbruch and R. H. Bube, *Fundamentals of Solar Cells* (Academic Press, Inc., New York, 1983).

[17] A. Luque and S. Hegedus, eds., *Handbook of Photovoltaic Energy Conversion and Engineering* (John Wiley & Sons Ltd, Chichester, West Sussex, England, 2003).

[18] X. Wu, J. C. Keane, R. G. Dhere, C. DeHart, D. S. Albin, A. Duda, T. A. Gessert, S. Asher, D. H. Levi, and P. Sheldon, in *Proc. 17th European Photovoltaic Sol. Energy Conf.* (NREL, 2001), pp. 995–1000.

[19] W. N. Shafarman and L. Stolt, *Handbook of Photovoltaic Science and Engineering* (Wiley Chichester, 2003), chap. Cu(In,Ga)Se$_2$ Solar Cells, pp. 567–616.

[20] L. J. Simpson, J. S. Britt, S. Wiedeman, M. E. Beck, B. S. Joshi, T. L. Vincent, J. P. Delplanque, R. J. Kee, N. B. Gomez, K. M. Williams, et al., NCPV and Solar Program Review Meeting p. 604 (2003).

[21] G. Jensen, J. Schaefer, G. M. Hanket, E. Eser, and S. Wiedeman, NCPV and Solar Program Review Meeting p. 877 (2003).

[22] R. Birkmire, E. Eser, S. Fields, and W. Shafarman, Prog. Photovoltaics **13**, 141 (2005).

[23] M. S. Keshner and R. Arya, Tech. Rep., National Renewable Energy Laboratory, http://www.nrel.gov/docs/fy05osti/36846.pdf (2004).

[24] M. A. Contreras, K. Ramanathan, J. AbuShama, F. Hasoon, D. L. Young, B. Egaas, and R. Noufi, Prog. Photovoltaics (in press) (2005).

[25] K. Ramanathan, M. A. Contreras, C. L. Perkins, S. Asher, F. S. Hasoon, J. Keane, D. Young, M. Romero, W. Metzger, R. Noufi, et al., Prog. Photovoltaics **11**, 225 (2003).

[26] K. Ramanathan, G. Teeter, J. C. Keane, and R. Noufi, Thin Solid Films, in press (2005).

[27] U. Rau and H. W. Schock, Appl. Phys. A **69**, 131 (1999).

[28] S. B. Zhang, S.-H. Wei, A. Zunger, and H. Katayama-Yoshida, Phys. Rev. B **57**, 9642 (1998).

[29] D. Rudmann, A. F. da Cunha, M. Kaelin, F. Kurdesau, H. Zogg, and A. N. Tiwari, Appl. Phys. Lett. **84**, 1129 (2004).

[30] C. R. Corwine, A. O. Pudov, M. Gloeckler, S. H. Demtsu, and J. R. Sites, Sol. Energy Mat. Sol. Cells **82**, 481 (2004).

[31] A. Pudov, Ph.D. thesis, Colorado State University (2005).

[32] A. Romeo, M. Terheggen, D. Abou-Ras, D. L. Bätzner, F.-J. Haug, M. Kälin, D. Rudmann, and A. N. Tiwari, Prog. Photovoltaics **12**, 93 (2004).

[33] K. L. Chopra, P. D. Paulson, and V. Dutta, Prog. Photovoltaics **12**, 69 (2004).

[34] J. R. Sites, H. Tavakolian, and R. A. Sasala, Solar Cells **29**, 39 (1990).

[35] M. Gloeckler and J. R. Sites, J. Appl. Phys. **95**, 4438 (2004).

[36] J. T. Heath, J. D. Cohen, and W. N. Shafarman, J. Appl. Phys. **95**, 1000 (2004).

[37] M. Burgelman, P. Nollet, and S. Degrave, Thin Solid Films **361-362**, 527 (2000).

[38] K. Emery, *Handbook of Photovoltaic Science and Engineering* (Wiley Chichester, A. Luque and S. Hegedus (Ed.), 2003), pp. 702–711 (Based on R. Bird, R. Hulstrom, and C. Riordan, Solar Cells 14, 193 [1985]).

[39] P. K. Johnson, Ph.D. thesis, Colorado State University (2003).

[40] S. S. Hegedus and W. N. Shafarman, Prog. Photovoltaics **12**, 155 (2004).

[41] J. R. Sites and P. H. Mauk, Solar Cells **27**, 411 (1989).

[42] *Personal correspondence with K. Ramanthan, M. Contreras, D. Albin, J. AbuShama, and S. Shaheen at the National Renewabel Energy Laboratory; J. Phillips; Gregory Parsons at NC State; available to others upon request.*

[43] M. Gloeckler and J. R. Sites, in *Proc. 19th European Photovoltaic Sol. Energy Conf.* (CSU, 2004).

[44] W. Shockley and W. T. R. Jr., Physical Review **87**, 835 (1952).

[45] R. N. Hall, Phys. Rev. **87**, 387 (1952).

[46] R. C. Neville, *Solar Energy Conversion: The solar cell* (Elsevier, New York, 1995).

[47] *ISE Integrated Systems Engineering Release 9.5 - Part 15: DESSIS*, ISE Integrated Systems Engineering AG, Zurich, Switzerland (2004).

[48] *A manual for AMPS-1D for Windows '95/NT*, Pennsylvania State University (1997).

[49] *Personal correspondence with W. K. Metzger, NREL.*

[50] D. Schmid, M. Ruckh, and H. W. Schock, Sol. Energy Mat. Sol. Cells **41-42**, 281 (1996).

[51] T. Schulmeyer, R. Hunger, A. Klein, W. Jaegermann, and S. Niki, Appl. Phys. Lett. **84**, 3067 (2004).

[52] S.-H. Wei and A. Zunger, Appl. Phys. Lett. **63**, 2549 (1993).

[53] F. Säuberlich and A. Klein, Mat. Res. Soc. Symp. Proc. **763**, 471 (2003).